ELSEVIER

Mathematical Biosciences 159 (1999) 123–144

Mathematical Biosciences
an international journal

www.elsevier.com/locate/mbs

Effective rate models for the analysis of transport-dependent biosensor data

Tamra Mason [a], Angel R. Pineda [b], Carla Wofsy [a], Byron Goldstein [c,*]

[a] *Department of Mathematics and Statistics, University of New Mexico, Albuquerque, NM 87131, USA*

[b] *Program in Applied Mathematics, University of Arizona, Tucson, AZ 85721, USA*

[c] *Theoretical Biology and Biophysics Group, Theoretical Division T-10, MS K710, Los Alamos National Laboratory, Los Alamos, NM 87545, USA*

Received 8 July 1998; received in revised form 4 March 1999; accepted 4 March 1999

Abstract

Optical biosensors, including the BIACORE, provide an increasingly popular method for determining reaction rates of biomolecules. In a flow chamber, with one reactant immobilized on a chip on the sensor surface, a solution containing the other reactant (the analyte) flows through the chamber. The time course of binding of the reactants is monitored. Scientists using the BIACORE to understand biomolecular reactions need to be able to separate intrinsic reaction rates from the effects of transport in the biosensor. For a model to provide a useful basis for such an analysis, it must reflect transport accurately, while remaining simple enough to couple with a routine for estimating reaction rates from BIACORE data. Models have been proposed previously for this purpose, consisting of an ordinary differential equation with 'effective rate coefficients' incorporating reaction and transport parameters. In this paper we investigate both the theoretical basis and numerical accuracy of these and related models.

Keywords: Biosensors; BIACORE; Mass transport; Binding kinetics; Diffusion-reaction

* Corresponding author. Tel.: +1-505 667 6538; fax: +1-505 665 3493; e-mail: bxg@lanl.gov

0025-5564/99/$ – see front matter
PII: S0025-5564(99)00023-1

1. Introduction

The first step for both cells and biosensors in detecting a specific ligand in solution is the binding of the ligand to a surface receptor. Because detection starts with the formation of a ligand–receptor complex on a surface, the kinetics of binding and dissociation may be influenced by the transport of the ligand to the surface. If the chemical reaction is slow compared to transport, the binding kinetics is unaffected by transport and the system acts as if it were well mixed. If the chemical reaction is fast, for example if the ligand–receptor forward rate constant or the receptor surface density is high, the binding kinetics will be affected or even dominated by transport.

Two of the best studied examples of transport-influenced binding kinetics are the binding of ligands to receptors uniformly distributed on spherical surfaces, cells or beads, where ligands are transported to the surface by diffusion alone [1–7] and the binding of ligands to receptors uniformly distributed on flat surfaces where, in addition to diffusion, ligands are transported by laminar flow parallel to the surface [8–14]. The latter occurs in the flow cell of the commercial optical biosensor, BIACORE. In this instrument, receptors are attached to a sensor surface and ligand, called the analyte, is injected at one end of the flow cell, flows past the sensor surface and exits at the other end. In comparing the effects of transport in these two cases there is an important distinction beyond the differences in the modes of transport themselves. In the case of the spherical cell the influence of transport is the same at all points on the surface. The probability of a receptor binding a ligand is independent of the position of the receptor on the sphere. Similarly the probability of a ligand dissociating from a receptor and escaping into the bulk solution rather than returning and rebinding to a surface receptor is the same for any ligand–receptor complex on the spherical surface. This is not true in the BIACORE flow cell, where transport depends on position. During association, ligands bind first to receptors near the influx channel. During dissociation, when buffer alone is injected into the flow cell, ligands that dissociate from receptors near the channel entrance have the highest probability of rebinding to a receptor before flow carries them to the channel exit.

We are interested in obtaining a simple, accurate description of the binding kinetics at the sensor surface of a BIACORE flow cell. Before discussing this problem, we review how binding has been modeled when ligands interact with receptors on spherical surfaces. We focus on a compartment model, reviewing how, under certain conditions, it yields a simple intuitive description of the binding kinetics in terms of a chemical rate equation with the true rate constants replaced by effective rate coefficients. Additional questions arise when one uses this compartmental approach to describe the binding kinetics in a BIACORE flow cell, where transport to the sensor surface is non-uniform.

To obtain a description of the analyte–receptor binding kinetics at the sensor surface, we start from a full description of the problem, a partial differential equation (PDE) that describes transport in the flow cell and boundary conditions that describe the influx and efflux of the analyte, the chemical reaction at the sensor surface, and the confinement of the analyte to the flow cell. We discuss the conditions under which this formulation leads to an effective rate description. Finally, we compare numerical solutions of the full description (PDE) with those for the effective rate description.

2. Background: compartment models

In studying the binding of ligands to receptors on surfaces, it is the binding kinetics that one is normally interested in. Thus, one is usually happy to abandon a detailed description of the spatial changes in the ligand concentration, in order to obtain a valid description of how the bound ligand concentration, B, changes with time. A popular approach for obtaining such a description is to approximate the continuous spatial change in the ligand concentration by dividing the volume outside the surface into discrete compartments, in each of which the ligand concentration is uniform. Consider the binding of diffusing ligands to receptors on a cell. In the standard approximation, the space outside the sphere is divided into two compartments as shown in Fig. 1(a), an outer compartment where the ligand concentration is that of the bulk solution, $\bar{C}$, and an inner compartment where the ligand concentration, C, changes because ligands bind to, and dissociate from, receptors and because ligands are transported to and from the outer compartment.

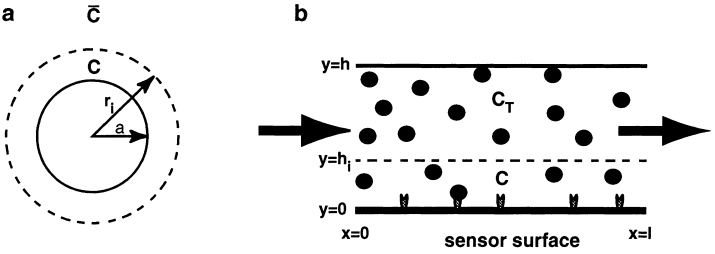

Fig. 1. (a) A compartment model for ligands binding to receptors on a spherical surface of radius a. The space outside the sphere is divided into an inner region, $a < r \leqslant r_i$, where the ligand concentration is C, and an outer region, $r > r_i$, where the ligand concentration equals the bulk concentration $\bar{C}$. (b) A compartment model for the flow cell of a BIACORE. In the compartment near the surface where the reaction takes place, $0 < y \leqslant h_i$, the analyte concentration is C, while in the outer region, $h_i < y \leqslant h$, the analyte concentration equals the injection concentration C_T.

Let us look at a single cell, with receptors distributed uniformly over its surface. At time $t = 0$, the ligand concentration is uniform, except in a small region about the cell (the inner compartment) where the concentration is 0, i.e., at $t = 0$, $\bar{C} = C_T$ for $r \geqslant r_i$ and $C = 0$ for $r_i > r \geqslant a$. Initially, ligands diffuse rapidly into the inner compartment and then bind to the cell surface receptors. Because the problem has radial symmetry, the net flux is only in the radial direction. We let V denote the volume of the inner compartment, A the surface area of the cell, and R the concentration of free receptors on the cell surface. Then the quantities VC, AR and AB are non-dimensional. The free ligand concentration C in the inner compartment and the bound ligand concentration B on the cell surface obey the following equations:

$$V\,\mathrm{d}C/\mathrm{d}t = -k_a ARC + k_d AB + k_+(\bar{C} - C) \tag{1}$$

$$\mathrm{d}B/\mathrm{d}t = k_a RC - k_d B, \tag{2}$$

where k_a and k_d are the fundamental rate constants for association and dissociation of a monovalent ligand with a receptor binding site, and k_+ is the rate constant that characterizes diffusion between the inner and outer compartment.

We now assume, and then justify, that after a short transient of duration t_t, during which there is negligible binding, the ligand concentration rises rapidly in the inner compartment and then changes slowly with time. If this is so, we can make a quasi-steady state approximation and set $\mathrm{d}C/\mathrm{d}t = 0$. When the left side of Eq. (1) is set equal to zero, one can solve for C and use the equation obtained to eliminate this variable from Eq. (2). This yields the following equation for B:

$$\mathrm{d}B/\mathrm{d}t = k_f^e R\bar{C} - k_r^e B, \tag{3}$$

where we have introduced effective forward and reverse rate coefficients

$$k_f^e = \frac{k_a}{1 + k_a RA/k_+} \qquad k_r^e = \frac{k_d}{1 + k_a RA/k_+}. \tag{4}$$

Since the total concentration of receptors, R_T, is conserved (we assume there is no internalization or degradation of receptors), we have $R = R_T - B$. With this conservation equation, and the initial condition $B(0) = 0$, Eq. (3) can be solved for B. If we are dealing with a single cell in an infinite volume, $\bar{C}$ will be constant and equal to C_T, since binding to the cell surface will not deplete the ligand. If there is a population of cells, with concentration ρ cells/ml, then $\bar{C} = C_T - AB\rho/(6.02 \times 10^{20})$, where the ligand concentrations are in molar (M).

We identify k_+ as the diffusion limited forward rate constant by letting the concentration of cell surface receptors become very large ($R \to \infty$) so that the reaction at the surface becomes instantaneous and the cell acts like a perfect absorber. In this limit the rate of reaction is determined by the rate at which ligands arrive at the surface due to diffusion and Eq. (3) becomes

$$\lim_{R\to\infty} \mathrm{d}B/\mathrm{d}t = k_+\bar{C}/A. \tag{5}$$

For two spherical particles whose radii sum to a and whose diffusion coefficients sum to D we have the Smoluchowski [15] result, that

$$k_+ = 4\pi Da. \tag{6}$$

For a molecule interacting with a cell, to an excellent approximation, a is the radius of the cell and D the diffusion coefficient of the ligand. Eq. (6) is obtained by solving the steady state diffusion equation with boundary conditions that at $r = a$, $C = 0$, and at $r = \infty$, $C = \bar{C}$, where the cell is centered at $r = 0$. The diffusion limited forward rate constant is obtained from the flux at the surface, i.e.,

$$k_+ = \frac{4\pi a^2 D}{\bar{C}} \left.\frac{\partial C(r)}{\partial r}\right|_{r=a}. \tag{7}$$

To estimate the duration of the transient, t_t, before the quasi-steady state approximation is valid we assume binding is negligible during this period and set $B = 0$ and $R = R_\mathrm{T}$ in Eq. (1). The solution C of the resulting equation increases with characteristic time

$$t_\mathrm{t} = V/(k_\mathrm{a}AR_\mathrm{T} + k_+). \tag{8}$$

An upper bound on the fraction of sites bound during time t_t is

$$B(t_\mathrm{t})/R_\mathrm{T} \leqslant k_\mathrm{a}\bar{C}t_\mathrm{t} \leqslant k_\mathrm{a}\bar{C}\ V/k_+. \tag{9}$$

One problem with the compartmental model is that the volume V of the inner compartment is unspecified. If we take it to be equal to the volume of the cell, and substitute k_+ from Eq. (6), then the upper bound in Eq. (9) becomes $k_\mathrm{a}\bar{C}a^2/(3D)$. If diffusion is fast, so that a^2/D, the characteristic time to diffuse the length of a cell radius, is short compared to the characteristic reaction time, $1/(k_\mathrm{a}\bar{C})$, there is negligible binding during the transient and we expect the effective rate description, Eqs. (3) and (4), to be an excellent approximation of the compartment model [16].

Although often done, using the same approach to model the binding kinetics of analyte flowing past, and interacting with, receptors immobilized on a sensor surface is more problematic (Fig. 1(b)). This is because during binding and dissociation, gradients in the analyte concentration arise that are both perpendicular (y direction) and parallel (x direction) to the flow. The concentration of bound analyte–receptor complex varies along the sensor surface in the x direction as does the transport limited forward rate constant. To a good approximation, the transport limited forward rate constant for a BIACORE flow cell, k_M, is

$$k_+(x)/A = k_\mathrm{M}(x) = \frac{1}{\Gamma(4/3)}\left(\frac{4v_\mathrm{c}D^2}{9hx}\right)^{1/3} \approx 0.855\left(\frac{v_\mathrm{c}D^2}{hx}\right)^{1/3}, \tag{10a}$$

where h is the height of the flow cell, l the length of the sensor surface, and v_c the flow velocity in the center of the flow cell [11]. Averaging Eq. (10a) over the length of the sensor surface we obtain

$$\langle k_M \rangle = \frac{1}{\Gamma(4/3)} \left(\frac{3 v_c D^2}{2hl} \right)^{1/3} \approx 1.282 \left(\frac{v_c D^2}{hl} \right)^{1/3}. \tag{10b}$$

It has usually been assumed that a compartment model for the flow cell can be used with k_+ in Eq. (4) simply replaced by the value of the transport coefficient averaged over x, i.e., by $A\langle k_M \rangle$. Is that correct? Also, if one is interested in how the bound analyte is distributed on the sensor surface as a function of position, can one simply replace k_+ by $Ak_M(x)$ as given by Eq. (10a)? Starting from a more complete description of the problem than a compartment model, we will answer these questions.

3. The full model

The PDE model for the BIACORE flow cell, which we present here as the standard for assessing the performance of simpler approximations, is based on a number of assumptions. We begin by discussing these assumptions, and the conditions under which they hold.

In a BIACORE flow cell, receptors can be coupled to the sensor surface in a variety of ways. We assume that the coupling immobilizes the receptor, but does not introduce any heterogeneities in the binding process. We assume the receptors are uniformly distributed on the sensor surface and act as binding sites on a two dimensional surface. If the receptors are distributed in a small volume above the sensor surface, we assume that the height of the layer does not influence the binding kinetics. Most often in a BIACORE, a CM5 sensor chip is used. Here receptors are coupled to uncrosslinked polymers of dextran which form a layer extending approximately $d = 1 \times 10^{-5}$ cm out from the sensor surface. This layer will not influence the binding kinetics and can be ignored when the average distance the analyte travels in the dextran layer before it binds to a receptor, its mean free path, is long compared to the height of the layer, d. If R_T is the surface concentration of receptors (receptors/cm^2), D_i is the diffusion coefficient of the analyte in the dextran layer, and k_a is the forward rate constant for analyte–receptor binding, then the layer can be ignored if $\sqrt{dD_i/(k_a R_T)} \gg d$.

In the flow cell, analyte is transported by diffusion and flow to the sensor surface where it reacts with immobilized receptors. The flow cell has a rectangular cross section. Standard dimensions are length $l = 0.24$ cm, width $w = 0.05$ cm, and height $h = 0.005$ cm. (In a new model, BIACORE 3000, h is reduced to less than half this height.) Binding is measured over a central rectangular portion of the chip, 0.016 cm wide and 0.14 cm long. We make two

approximations concerning the flow profile that are valid for most of the flow cell, in particular the region where binding is measured. First, we ignore any gradients that may arise along the width of the flow cell. We use the coordinate system shown in Fig. 1(b), with the x axis parallel to the direction of flow, and the y axis normal to the sensor surface. Brody et al. [17] show that for the specific aspect ratio $h/w = 0.1$, and in general for small aspect ratio h/w, the velocity profile in the y direction does not vary over most of the width of the chamber; the boundary layers at the chamber walls where the velocity drops to 0 extend less than h/w of the channel width. In the second approximation, we take the flow to be fully developed throughout the flow cell, so that the velocity profile is parabolic for $0 \leqslant x \leqslant l$, equal to zero at the top ($y = h$) and bottom ($y = 0$) boundaries, and maximal and equal to v_c in the center ($y = h/2$). The velocity $v(y)$ at a height y above the sensor surface is

$$v(y) = 4v_c(y/h)(1 - (y/h)). \tag{11}$$

Brody et al. [17] review results for a similar problem in a simpler geometry, i.e., a fluid entering a narrow cylindrical channel from a wider one, under conditions of low Reynolds number that are characteristic of the fluid dynamics of microdevices like the BIACORE flow cell. The flow becomes 99% fully developed over a distance on the order of the small radius. The analogous dimension in the BIACORE is the height of the flow cell, which is only 0.02 times the length of the flow cell. Both of the approximations we make in describing the flow profile were introduced by Lok et al. [11] and used in subsequent PDE models of the BIACORE [8,9,12,14,18,19].

In the flow channel, the analyte concentration $C(t,x,y)$ is governed by the following equation [12,18,19]:

$$\partial C/\partial t = D(\partial^2 C/\partial x^2 + \partial^2 C/\partial y^2) - 4v_c(y/h)(1 - (y/h))\partial C/\partial x \tag{12}$$

with boundary conditions:

$$\partial C(t,x,y)/\partial y = 0 \qquad \text{at } y = h, \tag{13a}$$

$$D\partial C(t,x,y)/\partial y = \partial B(t,x)/\partial t = k_a C(t,x,0)R(t,x) - k_d B(t,x) \quad \text{at} \quad y = 0, \tag{13b}$$

$$C(t,x,y) = C_T \qquad \text{at} \quad x = 0, \tag{13c}$$

$$\partial C(t,x,y)/\partial x = 0 \qquad \text{at} \quad x = l, \tag{13d}$$

$C(t,x,0)$ is the free analyte concentration at time t and position x, just above the sensor surface. $B(t,x)$ is the concentration of bound analyte–receptor complex on the cell surface and $R(t,x) = R_T - B(t,x)$ is the free surface receptor concentration. R_T is the total receptor concentration, which is constant with respect to both position and time. The rate constants for the reaction are k_a and k_d.

At the top boundary, $y = h$, the flux vanishes because the surface is impenetrable and unreactive. At the bottom boundary, $y = 0$, the flux into the

sensor surface equals the time rate of change in the amount of bound analyte at the surface.

At the flow cell inlet ($x = 0$) the analyte concentration is constant and equal to the injection concentration, C_T. At the outlet ($x = l$), we treat the exit of analyte as if it were due entirely to flow. Although this is an approximation, we will show later that the flow is fast compared to diffusion and therefore errors introduced by using Eq. (13d) propagate in the direction of flow, outside the computational domain, but have a negligible effect on the processes occurring in the flow cell.

4. Numerical solution of the full model

After Eqs. (12), (13a)–(13d) were nondimensionalized (see Section 5), the model was solved numerically by a method of lines algorithm. The diffusive terms were discretized using central differencing, and the convective term using first order up-winding. Several higher order schemes for strongly convective systems were tested against a highly resolved finite element solution. In these empirical tests, the first order discretization was comparable to the higher order schemes in terms of convergence and had the best stability properties. We think that this is tied to the implementation of the non-linear boundary condition. The time stepping was done with a midpoint scheme and an adaptive time step based on step doubling error checking. Higher order schemes in time were not necessary because of the stability constraints on the time step [20].

Because most of the variation in analyte concentration occurs near the sensor surface ($y = 0$), the domain was discretized using a non-uniform grid which concentrates the grid points near $y = 0$, as shown in Fig. 2. In the lower quarter of the grid, the distance between grid lines is half that for the upper portion of the grid.

The boundary conditions were implemented numerically by a first order discretization using ghost points. In numerical trials, higher order implementations failed to improve results.

At the point (0,0), the boundary conditions, Eqs. (13b) and (13c), require that $C = C_T$ and that $D\partial C(t,x,y)/\partial y = \partial B(t,x)/\partial t$. To resolve this conflict, we set $C = C_T$ at (0,0) and, for this single point, ignore the condition imposed by Eq. (13b). This results in a boundary layer in the numerical solution that did not propagate through the domain. We also implemented the boundary condition of Eq. (13b) instead of $C = C_T$ at (0,0) and found that our solution was independent of the implementation we picked.

The program was checked by comparing it with an existing code that used a finite element method to solve Eq. (12) numerically, subject to Eqs. (13a)–(13d) [12]. Convergence was also checked by comparing results on increasingly refined grids.

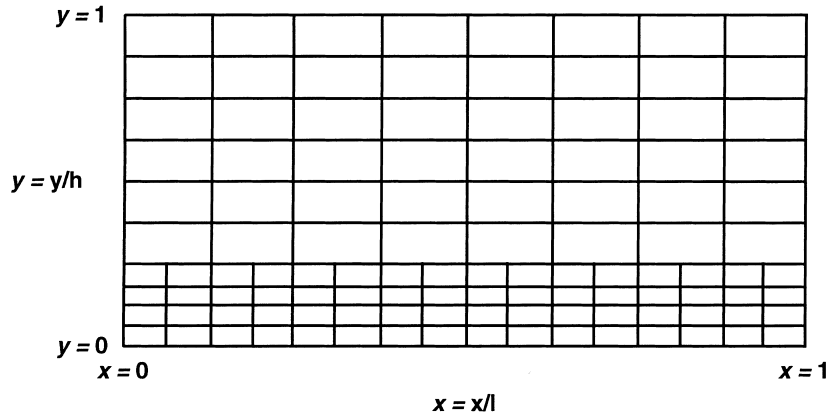

Fig. 2. Computational grid for an '8×8' discretization. By an '$n \times n$' grid we mean a grid constructed in the following manner: An $n \times n$ grid is formed with equal spacing between grid lines in both the horizontal and vertical directions. For the lower quarter of the domain the spacing between grid points is halved in both the x and y directions. For the points on the interface of the coarse and fine grid, $y = 1/4$, that do not fall on the coarse grid, linear interpolation is used to define the analyte concentration.

5. Derivations of effective rate models

To derive an approximate model for B, the amount of analyte bound to receptors on the sensor surface, we need an approximate expression for the concentration C of free analyte near the sensor surface. As in the case of binding to a spherical surface, we expect that there will be a brief transient during which the free analyte concentration will rise steeply but binding will be negligible, after which the analyte concentration will change slowly in time. Further, for the flow velocities used in a BIACORE, transport in the x direction will be dominated by flow and diffusion can be neglected, i.e., the characteristic time to diffuse the length of the flow cell is much longer than the time to transverse this distance by flow: $l^2/D \gg l/\bar{v}$ or equivalently, $1 \gg D/(l\bar{v})$ where $\bar{v} = 2v_c/3$ is the average flow velocity. In BIACORE experiments, $l = 0.24$ cm, $v_c = 1 - 10$ cm/s and $D < 10^{-5}$ cm^2/s, so that $3D/(2v_c l) < 10^{-4}$. Finally, since we are only interested in the concentration near the sensor surface, we can linearize the flow velocity. Making these approximations, the governing equation (12), becomes

$$0 = D\partial^2 C/\partial y^2 - 4v_c(y/h)\partial C/\partial x. \tag{14}$$

This equation was introduced in Ref. [11] and can be justified rigorously, using singular perturbation theory [18,19]. The justification is discussed in Appendix A .

Before proceeding we introduce the following non-dimensional quantities:

$$\tau \equiv Dt/h^2, \qquad x \equiv x/l, \qquad y \equiv y/h, \tag{15a}$$

$$c \equiv C/C_T, \qquad b \equiv B/R_T, \qquad r \equiv R/R_T, \tag{15b}$$

$$\kappa_a \equiv k_a C_T h^2/D, \qquad \kappa_d \equiv k_d h^2/D, \tag{15c}$$

$$\varepsilon = h/l, \qquad p = 4v_c h/D, \qquad \sigma = hC_T/R_T. \tag{15d}$$

Then Eq. (14) becomes

$$0 = \partial^2 c/\partial y^2 - \varepsilon p y \, \partial c/\partial x. \tag{16}$$

Once diffusion in the x direction is ignored, we can drop one boundary condition, Eq. (13d). Also, in solving Eq. (16), we replace the condition at the upper boundary, Eq. (13a), by the condition that the solution remains finite as y goes to infinity. By only considering the velocity near $y = 0$ and dropping the y^2 term in Eq. (11) we have already assumed that the top boundary does not influence the concentration of analyte at the sensor surface. We expect this to be a reasonable approximation when the flow in the x direction is fast compared to diffusion in the y direction, i.e., $l/v_c \ll h^2/D$ (or equivalently, the Peclet number $\mathrm{Pe} = v_c h^2/Dl \gg 1$), and analyte that is reflected from the upper boundary is carried to the exit of the flow cell before it can diffuse to the vicinity of the sensor surface and contribute to the analyte concentration near $y = 0$. This requirement is met in BIACORE experiments, where $\mathrm{Pe} > 10^2$. The remaining boundary conditions are

$$\begin{aligned} \sigma \partial c(\tau, x, y)/\partial y &= \partial b(\tau, x)/\partial \tau \\ &= \kappa_a c(\tau, x, 0)(1 - b(\tau, x)) - \kappa_d b(\tau, x) \quad \text{at } y = 0 \end{aligned} \tag{17a}$$

$$c(\tau, x, y) = 1 \qquad \text{at} \quad x = 0 \tag{17b}$$

Eq. (16) is linear, and so we can solve it, subject to the boundary conditions, to obtain the non-dimensional concentration c of free analyte at the sensor surface ($y = 0$). Let $\hat{c}$ denote the Laplace transform of c with respect to x and let s denote the transform variable. Then taking Laplace transforms in Eq. (16) and changing to the variables

$$\tilde{c}(\tau, s, \tilde{y}) = \hat{c}(\tau, s, y) - 1/s, \qquad \tilde{y} = (\varepsilon p s)^{1/3} y \tag{18}$$

we find that $\tilde{c}$ satisfies

$$0 = \partial^2 \tilde{c}/\partial \tilde{y}^2 - \tilde{y}\tilde{c}. \tag{19}$$

The solutions to Eq. (19) are Airy functions, $Ai(\tilde{y})$ and $Bi(\tilde{y})$ [21]. Since $Bi(\tilde{y})$ becomes infinite as $\tilde{y}$ becomes infinite, the solution to Eq. (19) that remains finite has the form $\tilde{c} = aAi(\tilde{y})$. Then

$$\hat{c}(\tau, s, y) = 1/s + aAi((\varepsilon p s)^{1/3} y). \tag{20}$$

We obtain the constant a from the Laplace transform in x of the boundary condition at $y = 0$, Eq. (17a), and find that

$$\hat{c}(\tau, s, 0) = \frac{1}{s} - \frac{c_1 \hat{\dot{b}}}{c_2 \sigma (\varepsilon p s)^{1/3}}, \tag{21}$$

where [21]

$$c_1 = Ai(0) = 1/(3^{2/3}\Gamma(2/3)) \approx 0.35502, \tag{22a}$$

$$c_2 = -Ai'(0) = 1/(3^{1/3}\Gamma(1/3)) \approx 0.25881, \tag{22b}$$

and $\dot{b} = \partial b(\tau, x)/\partial \tau$. Inverting the Laplace transform in Eq. (21) we obtain

$$c(\tau, x, 0) = 1 - \frac{c_1}{c_2 \sigma \Gamma(1/3)(\varepsilon p)^{1/3}} \int_0^x \dot{b}(\tau, u)(x-u)^{-2/3}\,\mathrm{d}u. \tag{23}$$

Finally, substituting for c in Eq. (17a) we obtain an integro-differential equation for the non-dimensional concentration of bound analyte

$$\dot{b} = \kappa_a \left(1 - \frac{c_1}{c_2 \sigma \Gamma(1/3)(\varepsilon p)^{1/3}} \int_0^x \dot{b}(\tau, u)(x-u)^{-2/3}\mathrm{d}u\right)(1-b) - \kappa_\mathrm{d} b. \tag{24}$$

In Section 6, we show that predictions of the time course of analyte binding and dissociation in a BIACORE experiment, based on Eq. (24), match predictions of the full PDE model (Eqs. (12), (13a)–(13d)) closely, for parameters ranging from the diffusion-limited regime through the reaction-limited case.

Although Eq. (24) gives an accurate approximation to the full model and can be solved much more rapidly (see Appendix B for the numerical scheme), an accurate effective rate approximation would be even simpler to use. We now turn to the derivation of two effective rate models, one that gives the approximate concentration of bound analyte as a function of position x in the direction of flow, and one that gives the approximate concentration averaged over x.

If we expand $\dot{b}(\tau, u)$ in Eq. (24) in a power series in u, about $u = x$, and simply keep the first term, i.e., ignore all spatial derivatives and set

$$\int_0^x \dot{b}(\tau, u)(x-u)^{-2/3}\,\mathrm{d}u \approx 3x^{1/3}\dot{b}(\tau, x) \tag{25}$$

then we obtain an equation for $b(\tau, x)$ in the form of a standard chemical rate equation. In dimensional form, we have Eq. (3) for $B(t, x)$, with effective rate coefficients

$$k_{\mathrm{f}}^{\mathrm{e}} = \frac{k_{\mathrm{a}}}{1 + k_{\mathrm{a}}(R_{\mathrm{T}} - B)/(\beta k_{\mathrm{M}}(x))}, \quad k_{\mathrm{r}}^{\mathrm{e}} = \frac{k_{\mathrm{d}}}{1 + k_{\mathrm{a}}(R_{\mathrm{T}} - B)/(\beta k_{\mathrm{M}}(x))}, \tag{26a}$$

where $k_{\mathrm{M}}(x)$ is given by Eq. (10a) and

$$\beta \approx \Gamma(4/3)\Gamma(2/3) \approx 1.209. \tag{26b}$$

Since the output of a BIACORE, in its current form, is a spatial average of the concentration of bound analyte, it is reasonable to look for an effective rate equation for $\langle b \rangle$, the average of b over x. From Eq. (17a) we see that

$$\langle \dot{b} \rangle = \kappa_{\mathrm{a}} \langle c(\tau, x, 0)(1 - b(\tau, x)) \rangle - \kappa_{\mathrm{d}} \langle b(\tau, x) \rangle. \tag{27}$$

Note that

$$\langle cb \rangle = \langle c \rangle \langle b \rangle + \langle (c - \langle c \rangle)(b - \langle b \rangle) \rangle. \tag{28}$$

We ignore the second term in Eq. (28) and make the approximation that

$$\langle c(\tau, x, 0) b(\tau, x) \rangle = \langle c(\tau, x, 0) \rangle \langle b(\tau, x) \rangle. \tag{29}$$

Eq. (29) is exact at $t = 0$, when $c = 0$, and, if binding is allowed to reach equilibrium, at long times, when b is uniform. If dissociation is initiated when the system has reached equilibrium, again Eq. (29) is exact at the beginning and end of the process. In the reaction limit, when transport is rapid compared to binding, c is essentially uniform and Eq. (29) holds for all time. Then from Eqs. (27) and (29),

$$\langle \dot{b} \rangle = \kappa_{\mathrm{a}} \langle c \rangle (1 - \langle b \rangle) - \kappa_{\mathrm{d}} \langle b \rangle \tag{30}$$

To obtain an equation for $\langle b \rangle$ we need an expression for $\langle c \rangle$. We replace $\dot{b}$ by its average, $\langle \dot{b} \rangle$, in Eq. (21) or, equivalently, in Eq. (23), and then average c over x. The resulting expression can now be substituted into Eq. (30) to give an ordinary differential equation for the average concentration of bound analyte. When the equation is written in dimensional form, we recognize the following analogue of Eq. (3):

$$\mathrm{d}\langle B \rangle / \mathrm{d}t = k_{\mathrm{f}}^{\mathrm{e}} (R_{\mathrm{T}} - \langle B \rangle) C_{\mathrm{T}} - k_{\mathrm{r}}^{\mathrm{e}} \langle B \rangle \tag{31}$$

with effective rate coefficients:

$$\begin{aligned} k_{\mathrm{f}}^{\mathrm{e}} &= \frac{k_{\mathrm{a}}}{1 + k_{\mathrm{a}}(R_{\mathrm{T}} - \langle B \rangle)/(\alpha \langle k_{\mathrm{M}} \rangle)}, \\ k_{\mathrm{r}}^{\mathrm{e}} &= \frac{k_{\mathrm{d}}}{1 + k_{\mathrm{a}}(R_{\mathrm{T}} - \langle B \rangle)/(\alpha \langle k_{\mathrm{M}} \rangle)}. \end{aligned} \tag{32a}$$

The transport coefficient $\langle k_{\mathrm{M}} \rangle$ is given by Eq. (10b) and

$$\alpha = (4/3)\Gamma(4/3)(2/3)\Gamma(2/3) \approx 1.075. \tag{32b}$$

Except for the small numerical correction, the constant α multiplying $\langle k_{\mathrm{M}} \rangle$, this is identical to the result obtained with a two compartment model [12].

In Section 6 we see how solutions to the effective rate models, with effective rate coefficients given by Eq. (26a) or Eq. (32a), compare with the numerical solution of the full PDE, Eq. (12).

6. Comparisons of approximate equations with numerical solutions of the full model

We compared solutions of each approximate model with the solution to the full PDE model for binding and transport in a BIACORE (Eqs. (12), (13a)–(13d)), focussing on conditions where we expect transport to influence binding. To ensure that the solutions to the full model are sufficiently accurate to make such comparisons, we first compared numerical solutions using different grids. For a wide range of feasible parameters, there is a negligible difference between a 96×96 and a 128×128 grid. In the remainder of this section we compare the approximate models to numerical solutions of the full model using a 96×96 grid.

First we see how well the approximate models do in predicting the average concentration of bound analyte as a function of time. The parameters used in the simulations in Fig. 3 were chosen so that the binding kinetics would be dominated by transport. From the form of Eq. (4), Eq. (10a) and Eq. (10b) it follows that when $k_aR/\langle k_M\rangle \gg 1$ the binding kinetics is determined by transport while when $k_aR/\langle k_M\rangle \ll 1$ the binding kinetics is determined by the chemical reaction. For the parameters used in Fig. 3, $k_aR_T/\langle k_M\rangle = 29.8$, so that at the start of the simulation, the binding is limited by transport of analyte to the sensor surface.

In Fig. 3(a) and Fig. 3(b) the solid line is the solution obtained from the full PDE model. The dotted line in Fig. 3(b) is the solution for a well mixed system, i.e., it is the solution to Eq. (3) with $k_f^e = k_a$ and $k_r^e = k_d$. We will call this the rapid mixing model. Comparing the dotted and solid curve in Fig. 3(b) we see the dramatic difference between the transport limited and the reaction limited binding kinetics. In the 60 s period of association, transport effects slow the forward kinetics so that binding remains far from equilibrium, whereas the rapid mixing model predicts rapid equilibration. The dotted line in Fig. 3(a) is the solution to the integro-differential equation, Eq. (24), averaged over x. That it is in good agreement with the full PDE model shows that for the parameters used in Fig. 3, approximating the full PDE, Eq. (12), by Eq. (14), i.e., setting $\partial C/\partial t = 0$ and ignoring diffusion in the x direction, is an excellent approximation. We have also compared two forms of the effective rate model for $\langle B\rangle$. The dash–dot curve in Fig. 3(a) is the solution to the ordinary differential equation, Eq. (3), with effective rate coefficients given by Eqs. (32a) and (32b). The dashed curve in Fig. 3 (b) is the solution to the same equation, but with $\alpha = 1$ rather than 1.075. It is the equation obtained from the two compartment

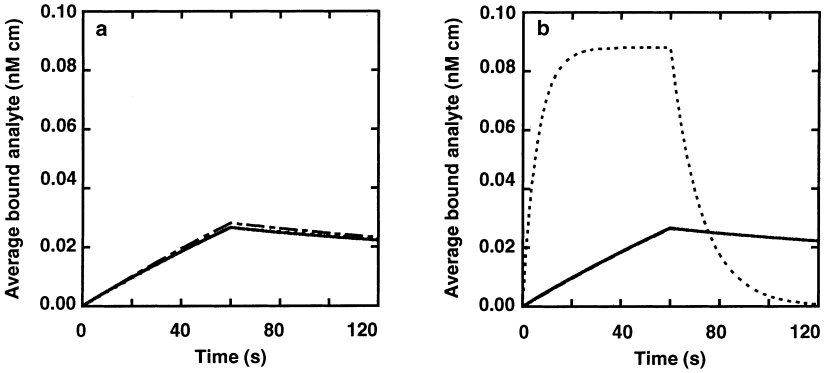

Fig. 3. Simulation of binding kinetics in the transport limit. Predictions of the time development of the average bound analyte concentration are plotted, for the following parameter values: $k_a = 1 \times 10^8$ M^{-1} s^{-1}, $k_d = 8 \times 10^{-2}$ s^{-1}, $D = 1 \times 10^{-7}$ cm ^{2}/s, $v_c = 10$ cm/s and $R_T = 1.67 \times 10^{-10}$ M cm. $C_T = 0.889$ nM for the first 60 s (binding phase) and zero for the last 60 s (dissociation phase). (a) The solid line is the solution to the full model, Eq. (12) and Eqs. (13a)–(13d). The dotted line, which is almost indistinguishable from the solid line, is the solution to the integro-differential equation, Eq. (24), averaged over x. The dash–dot line is the solution to the ordinary differential equation, Eq. (3), with effective rate coefficients given by Eqs. (32a) and (32b). (b) As in (a), the solid line is the solution to the full model. The dashed line is the solution to Eq. (3), with effective rate coefficients given by Eq. (32a), but with $\alpha = 1$ rather than 1.075. The dotted line is the solution for the rapid mixing model, Eq. (3) with the true rate constants rather than the effective rate coefficients.

model by requiring that in the transport limit, Eq. (5) is satisfied. It is therefore not surprising that since we are in this limit, choosing the effective rate constant in this way works so well.

In Fig. 4 we consider the case where transport influences the binding kinetics, but to a lesser degree than in Fig. 3. The parameters used in the simulations in Fig. 4 give $k_a R_T/\langle k_M \rangle = 1.92$, approximately 15 times smaller than in Fig. 3. Again, by comparing the solid line in Fig. 4(b), the full PDE model, with the dotted line, the rapid mixing model, we see that transport has a significant influence on the binding kinetics. Using the effective rate coefficients given by Eq. (32a) with $\alpha = 1.075$ we now get better agreement (dash–dot curve in Fig. 4(a)) with the solution to the full PDE model than when we set $\alpha = 1$ (dashed curve in Fig. 4 (b)). There is no single best choice for the value of α. For $k_a R_T/\langle k_M \rangle \gg 1$, $\alpha = 1$ is best, but when $k_a R_T/\langle k_M \rangle \approx 2$, $\alpha = 1.075$ gives better results. Of course when $k_a R_T/\langle k_M \rangle \ll 1$, the effective rate coefficients reduce to the true rate constants and the choice of α is irrelevant. Results of other simulations, with the analyte concentration varying over 2 orders of magnitude ($C_T = 0.0988$ nM – 8.0 nM), give the same trends and similar accuracy.

In Fig. 5 we show snap shots in time of the predicted distribution of free analyte in the flow cell, for the two cases we have discussed and whose

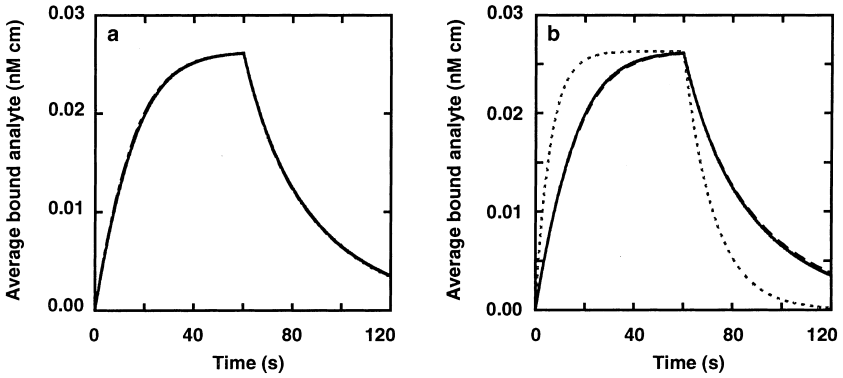

Fig. 4. Simulation of transport-influenced binding kinetics. To reduce the influence of transport in these simulations, relative to the case simulated in Fig. 3, the diffusion coefficient of the analyte was increased by a factor of ten, $D = 1 \times 10^{-6}$ cm^2/s, and the receptor density was decreased by a factor of 3.3, $R_T = 5 \times 10^{-11}$ M cm. All other parameters are the same as in Fig. 3 and the same comparisons are made. Although the solutions to both the full model and the integro-differential equation are plotted in panel (a), on this scale they are indistinguishable.

simulations are shown in Fig. 3 and Fig. 4. For the diffusion limited case, Fig. 5(a), we see that a strong gradient exists at 20 s. This gradient continues to exist until dissociation is initiated at 60 s (simulation not shown). For the case where transport influences the kinetics but to a lesser degree, Fig. 5(b), the gradient can be seen to dissipate in time and by 40 s (not shown) the analyte concentration is essentially uniform throughout the flow cell. The upper boundary only influences the distribution of analyte at very short times. In both cases, by 1 s the analyte concentration is uniform over more than 80% of the flow cell.

Although the current output of the BIACORE is a time course of the average concentration of bound analyte, it is possible that in the future, biosensors will yield concentrations at different locations along the sensor surface. Fig. 6 compares the time courses predicted for $x = 0.25$ by the full model and the effective rate model with spatial dependence, Eq. (3) with effective rates given by Eq. (26a) and $\beta = 1.209$ or $\beta = 1$. (Comparisons at $x = 0.50$ and 0.75 were also done with similar results.) The same trends as were seen in Figs. 3 and 4 are seen again. Both approximations give predictions that are close to those of the full model. In the transport limit, Fig. 6(a), the effective rate model with $\beta = 1$ is closer to the full model. In Fig. 6(b) when both transport and reaction contribute to the kinetics, the choice of $\beta = 1.209$ gives the more accurate approximation. As expected, during the association phase binding is higher close to the inlet than downstream (simulations not shown). In contrast, during the dissociation phase binding decreases more rapidly near the inlet and more slowly downstream, because analyte that dissociates from receptors flow away from the inlet and may rebind, closer to the outlet of the chamber.

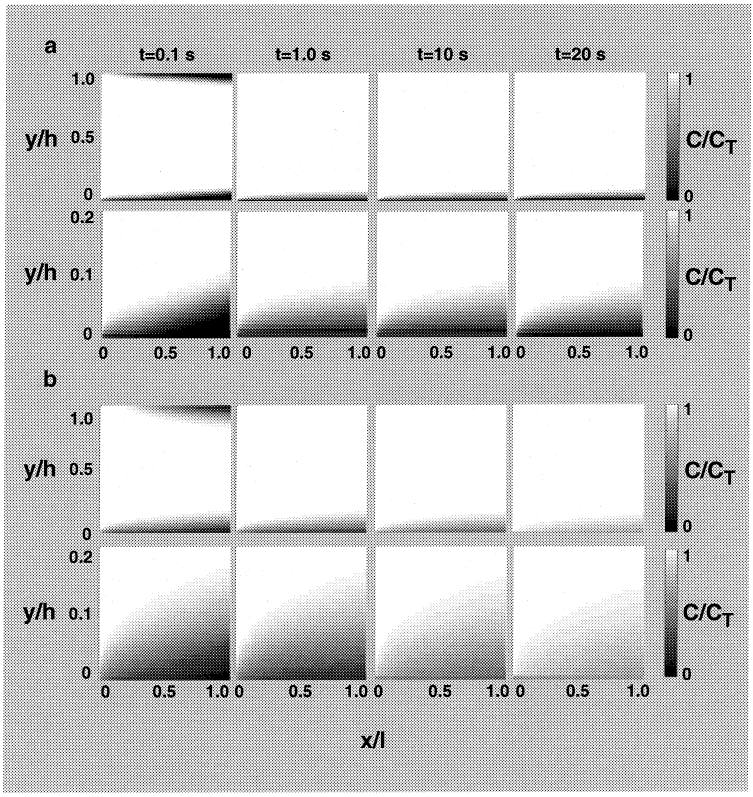

Fig. 5. The predicted distribution of analyte in the flow cell for 0.1, 1.0, 10 and 20 s after the start of binding. Black corresponds to an analyte concentration of zero and white to an analyte concentration equal to the injection concentration. In (a) and (b), the top panels show the entire flow cell while the bottom panels show the 20% of the flow cell above the reacting surface. (a) The diffusion-limited case, where parameters are given in Fig. 3. (b) The diffusion-influenced case, where parameters given in Fig. 4.

7. Discussion

A spectrum of models is available for the determination of fundamental parameters from BIACORE data. The simplest omits potential effects of flow and diffusion of the analyte by assuming that the concentration of the analyte is uniform throughout the flow cell and doesn't change with time. This model can be thought of as a 'rapid mixing' model. On the other end of the spectrum is the partial differential equation model given by Eq. (12) and Eqs. (13a)–(13d) that accounts fully for transport and binding. This 'full' model provides a standard against which to test approximations, but is not a feasible tool for extracting parameters that give the best fit of the model to data.

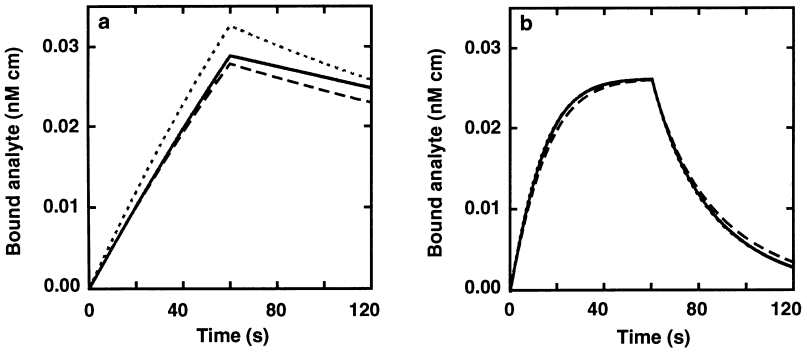

Fig. 6. Predictions of the time development of the bound analyte concentration at x = 0.25. Shown are the time courses predicted by the full model and the effective rate model with spatial dependence. The parameters used in panels a and b are the same as those used in Figs. 3 and 4, respectively. The solid line is the solution of the full model. The two other curves are solutions to the effective rate model with spatial dependence, Eq. (3) with effective rates given by Eq. (26a) and $\beta =$ 1.209 (dotted) or $\beta = 1$ (dashed).

A model that is easy to implement in a laboratory setting consists of an ordinary differential equation for the concentration of bound analyte, using effective forward and reverse rate coefficients that capture the effects of diffusion and flow. The general form of such a model for the concentration B of analyte bound to receptors with a total concentration R_T, on a surface of area A, is

$$dB/dt = \frac{k_a}{1 + k_a(R_T - B)A/k_+}(R_T - B)\bar{C} - \frac{k_d}{1 + k_a(R_T - B)A/k_+}B, \qquad (33)$$

where k_a and k_d are fundamental rate constants for association and dissociation and $\bar{C}$ is the concentration of ligand far from the surface where binding occurs. All of the information in the model concerning the transport of ligand and the geometry of the system resides in the constant k_+.

Compartmental models can lead to such a formulation, as we illustrated in the case of ligands binding to receptors on spherical cells or beads (where k_+ is identified as a diffusion- limited forward rate constant), and as demonstrated in [12] for the flow chamber of a biosensor.

We have asked, starting not from a compartmental model but from the full model, what form of k_+ is an appropriate choice for an effective rate constant model giving: (1) the concentration of bound analyte as a function of position and time, $B(t,x)$, or (2) the average concentration of bound analyte, $\langle B \rangle$, as a function of time, in a BIACORE flow cell? The expressions we obtained are given in Eqs. (26a) and (26b) and Eqs. (32a) and (32b), respectively. We have shown in simulations (Figs. 3, 4 and 6) that both models are close to the full model in their predictions of binding kinetics.

In the case of the model for $\langle B \rangle$, our results are close to those of Myszka et al. [12], derived from the two-compartment model, the expressions for k_+ differing by a factor of 1.075. The two expressions differ slightly in their predictions for $\langle B \rangle$. Myszka et al. [12] showed that using their model, they could recover parameters from data that were simulated based on the full model, with or without noise. Note that if Eq. (33) is used to fit BIACORE binding data and obtain estimates for the fundamental rate constants, k_+ will be treated as a free parameter and the choice of the factor will be irrelevant. Using this approach has been highly successful in fitting experimental data and determining k_a and k_d [22,23]. In the latest software supplied with the BIACORE instrument, BIAevaluation 3.0, the two compartment model, Eqs. (1) and (2), from which Eq. (33) follows, is available for fitting data.

We have also considered a second model which provides a good approximation for the concentration of bound analyte as a function of position in the direction of flow in a biosensor. The present generation of BIACORE instruments reports a spatial average of the concentration of bound analyte. If a next generation of biosensors is developed that obtains spatial data, this model can serve as a simple tool in its analysis.

Acknowledgements

The authors are grateful to Pedro Embid for key suggestions. This work was supported by National Science Foundation Grants MCB9723897 and HRD9627118, National Institutes of Health Grant GM35556 and the Los Alamos National Laboratory LDRD program.

Appendix A

In this section we outline the use of perturbation methods to derive Eq. (14), or equivalently, its non-dimensional form, Eq. (16), from Eq. (12). We non-dimensionalize according to Eqs. (15a)–(15d). The time scale implicit in the definition of τ is that of diffusion in the vertical direction (i.e., h^2/D is the characteristic time for a molecule to diffuse a distance equal to the height of the BIACORE). Then Eq. (12) becomes

$$\frac{\partial c}{\partial \tau} = \varepsilon^2 \frac{\partial^2 c}{\partial x^2} + \frac{\partial^2 c}{\partial y^2} - \varepsilon p y(1-y)\frac{\partial c}{\partial x}. \tag{A.1}$$

The product εp is related to the Peclet number, Pe:

$$\mathrm{Pe} = \varepsilon p/4 = \frac{h^2/D}{l/v_c} = \frac{\text{characteristic diffusion time in } y}{\text{characteristic convection time in } x}.$$

As already noted, for BIACORE experiments, $\mathrm{Pe} > 10^2$ and the aspect ratio $\varepsilon = h/l = 0.02$.

In order to do a boundary layer analysis near the sensor surface, we define a new variable to stretch the y coordinate, $\eta = y/\delta$. Then from Eq. (A.1), the inner solution, c^{i}, satisfies

$$\delta^2 \frac{\partial c^{\mathrm{i}}}{\partial \tau} = \delta^2 \varepsilon^2 \frac{\partial^2 c^{\mathrm{i}}}{\partial x^2} + \frac{\partial^2 c^{\mathrm{i}}}{\partial \eta^2} - \varepsilon p \delta^3 \eta (1 - \delta\eta) \frac{\partial c^{\mathrm{i}}}{\partial x}. \tag{A.2}$$

To keep the convection term, let $\delta = (\varepsilon p)^{-1/3}$. Then the zero order term, c_0, in the expansion for c^i as a power series in δ satisfies the partial differential equation

$$0 = \frac{\partial^2 c_0(\tau, x, \eta)}{\partial \eta^2} - \eta \frac{\partial c_0(\tau, x, \eta)}{\partial x}. \tag{A.3}$$

To express Eq. (A.3) in terms of y, recall that $\eta = y\delta = y(\varepsilon p)^{-1/3}$. Substitution for η in Eq. (A.3) yields Eq. (16).The outer solution, c^{o}, away from the boundary layer, satisfies Eq. (A.1) with δ substituted for $(\varepsilon p)^{-1/3}$. To lowest order in δ, the equation is

$$\frac{\partial c^{\mathrm{o}}}{\partial x} = 0.$$

Subject to the boundary condition $c^{\mathrm{o}} = 1$ at $x = 0$, the outer solution is constant, $c^{\mathrm{o}} = 1$. For the inner and outer solutions to match, the inner solution must approach 1 as $\eta \to \infty$.

Appendix B

In this Appendix, we describe the procedure we used for solving the integro-differential equation, Eq. (24), numerically. Define an operator T by

$$Tg(\tau, x) = \alpha(1 - b(\tau, x)) \int_0^x (x - s)^{-2/3} g(\tau, s)\, \mathrm{d}s, \tag{B.1}$$

where

$$\alpha = c_1 \kappa_{\mathrm{a}} / (c_2 \Gamma(1/3) \sigma (\varepsilon p)^{1/3}) \tag{B.2}$$

and the function b, the constants c_1 and c_2, and the non-dimensional parameters are as defined in Eqs. (15a)–(15d) and Eqs. (22a) and (22b). Then Eq. (24) can be rewritten as

$$(I + T)\dot{b} = \kappa_{\mathrm{a}} - (\kappa_{\mathrm{a}} + \kappa_{\mathrm{d}})b.$$

Under the assumption that $(I + T)^{-1}$ exists,

$$\dot{b} = (I + T)^{-1}(\kappa_{\mathrm{a}} - (\kappa_{\mathrm{a}} + \kappa_{\mathrm{d}})b). \tag{B.3}$$

Let Δx and $\Delta\tau$ denote the sizes of steps in space and time. Discretizing the time derivative in Eq. (B.3), we obtain

$$b(\tau+\Delta\tau,x)\approx b(\tau,x)+\Delta\tau f(\tau,x) \tag{B.4}$$

where

$$f(\tau,x)=(I+T)^{-1}(\kappa_{\mathrm{a}}-(\kappa_{\mathrm{a}}+\kappa_{\mathrm{d}})b(\tau,x)). \tag{B.5}$$

In order to approximate the right-hand side of Eq. (B.4) at $\mathrm{x}_i=i\Delta x$, $i=0,\ldots,n$, we use Eq. (B.5) in the form

$$(I+T)f(\tau,x_i)=\kappa_{\mathrm{a}}-(\kappa_{\mathrm{a}}+\kappa_{\mathrm{d}})b(\tau,x_i) \tag{B.6}$$

to obtain a system of linear equations that can be solved for the $f(\tau,x_i)$. To approximate the integral in Tf (Eq. (B.1)), at a point x_j, we write

$$\int_0^{x_j}(x_j-s)^{-2/3}f(\tau,s)\mathrm{d}s\approx\sum_{i=1}^{j}\int_{x_i}^{x_{i+1}}f(\tau,s)(x_j-s)^{-2/3}\mathrm{d}s.$$

In evaluating the integrals, we approximate $f(\tau,s)$ linearly on each of the subintervals $[x_i,x_{i+1}]$, i.e.,

$$f(\tau,s)\approx(\Delta x)^{-1}((f(\tau,x_i)(x_{i+1}-s)+(f(\tau,x_{i+1})(s-x_i))\qquad\text{on }(x_i,x_{i+1})$$

Then the matrix equation to solve for the $f(\tau,x_i)$ is

$$\begin{bmatrix}a_{0,0}&0&0&\cdots&0\\a_{1,0}&a_{1,1}&0&\cdots&0\\\vdots&\vdots&\vdots&&\vdots\\a_{n,0}&a_{n,1}&a_{n,2}&\cdots&a_{n,n}\end{bmatrix}\begin{bmatrix}f(\tau,x_0)\\f(\tau,x_1)\\\vdots\\f(\tau,x_n)\end{bmatrix}=\begin{bmatrix}\kappa_{\mathrm{a}}-(\kappa_{\mathrm{a}}+\kappa_{\mathrm{d}})b(\tau,x_0)\\\kappa_{\mathrm{a}}-(\kappa_{\mathrm{a}}+\kappa_{\mathrm{d}})b(\tau,x_1)\\\vdots\\\kappa_{\mathrm{a}}-(\kappa_{\mathrm{a}}+\kappa_{\mathrm{d}})b(\tau,x_n)\end{bmatrix},$$

where, if $\beta(x_i)=\alpha(1-b(\tau,x_i))$, the entries in the matrix are

$$a_{j,0}=\beta(x_j)(\Delta x)^{-1}\int_{x_0}^{x_1}(x_j-s)^{-2/3}(x_1-s)\mathrm{d}s,$$

$$a_{j,k}=\beta(x_j)(\Delta x)^{-1}\left(\int_{x_{k-1}}^{x_k}(x_j-s)^{-2/3}(s-x_{k-1})\mathrm{d}s+\int_{x_k}^{x_{k+1}}(x_j-s)^{-2/3}(x_{k+1}-s)\mathrm{d}s\right)\quad 1\leqslant k\leqslant j-1,$$

$$a_{j,j}=1+\beta(x_j)(\Delta x)^{-1}\int_{x_{j-1}}^{x_j}(x_j-s)^{-2/3}(s-x_{j-1})\mathrm{d}s,$$

$$a_{j,k}=0\qquad j<k.$$

Each of the integrals can be evaluated in terms of the x_i. Starting with the fact that $b(0,x_i) = 0$ for all i, we find the $f(0,x_i)$. For any τ, once we know $f(\tau,x_i)$ for all i, we update the bound ligand function, i.e., use Eq. (B.4) to find $b(\tau + \Delta\tau, x_i)$.

References

[1] H.C. Berg, E.M. Purcell, Physics of chemoreception, Biophys. J. 20 (1977) 193.
[2] O.G. Berg, On diffusion-controlled dissociation, Chem. Phys. 20 (1978) 47.
[3] C. DeLisi, F.W. Wiegel, Effect of nonspecific forces and finite receptor number on rate constants of ligand–cell bound-receptor interactions, Proc. Nat. Acad. Sci. USA 78 (1981) 5569.
[4] J. Erickson, B. Goldstein, D. Holowka, B. Baird, The effect of receptor density on the forward rate constant for binding of ligands to cell surface receptors, Biophys. J. 52 (1987) 657.
[5] B. Goldstein, M. Dembo, Approximating the effects of diffusion on reversible reactions at the cell surface: ligand–receptor kinetics, Biophys. J. 68 (1995) 1222.
[6] M. Schwartz, The adsorption of coliphage to its host: effect of variations in the surface density of receptor and in phage–receptor affinity, J. Molec. Biol. 103 (1976) 521.
[7] D. Shoup, A. Szabo, Role of diffusion in ligand binding to macromolecules and cell-bound receptors, Biophys. J. 40 (1987) 33.
[8] L.L.H. Christensen, Theoretical analysis of protein concentration determination using biosensor technology under conditions of partial mass transport limitation, Anal. Biochem. 249 (1997) 153.
[9] R.W. Glaser, Antigen–antibody binding and mass transport by convection and diffusion to a surface: a two-dimensional computer model of binding and dissociation kinetics, Anal. Biochem. 213 (1993) 152.
[10] R. Karlsson, H. Roos, L. Fägerstam, B. Persson, Kinetic and concentration analysis using BIA technology, Methods: A Companion to Methods Enzymol. 6 (1994) 99.
[11] B.K. Lok, Y.-L. Cheng, C.R. Robertson, Protein adsorption on crosslinked polydimethylsiloxane using total internal reflection fluorescence, J. Colloid Interface Sci. 91 (1983) 104.
[12] D.G. Myszka, X. He, M. Dembo, T.A. Morton, B. Goldstein, Extending the range of rate constants available from BIACORE: interpreting mass transport influenced binding data, Biophys. J. 75 (1998) 583.
[13] P. Schuck, Use of surface plasmon resonance to probe the equilibrium and dynamic aspects of interactions between biological macromolecules, Ann. Rev. Biophys. Biomol. Struct. 26 (1997) 541.
[14] M.L. Yarmush, D.B. Patankar, D.M. Yarmush, An analysis of transport resistances in the operation of BIACORE; Implications for kinetic studies of biospecific interactions, Molec. Immunol. 33 (1996) 1203.
[15] M.V. Smoluchowski, Versuch einer mathematischen theorie der kiagulationskinetik kolloider lösugen, Z. Phys. Chem. 92 (1917) 129.
[16] L.A. Segel, M. Slemrod, The quasi-steady-state assumption: a case study in perturbation, SIAM Rev. 31 (1989) 446.
[17] J.P. Brody, P. Yager, R.E. Goldstein, R.H. Austin, Biotechnology at low Reynolds numbers, Biophys J. 71 (1996) 3430.
[18] D.A. Edwards. Estimating rate constants in a convection- diffusion equation with a boundary reaction, IMA J. Appl. Math. (in press).
[19] D.A. Edwards, B. Goldstein, D.S. Cohen, Transport effects on surface-volume biological reactions, J. Math. Biol. (in press).

[20] K.W. Morton, Numerical Solution of Convection–Diffusion Problems, Chapman and Hall, London, 1996.
[21] M. Abramowitz, I.A. Stegun, (Eds.), Handbook of Mathematical Functions, National Bureau of Standards, Washington DC, 1964, p. 446.
[22] D.G. Myszka, P.R. Arulanantham, Z. Wu, T. Sana, T.L. Ciardelli, Kinetic analysis of ligand binding to interleukin-2 receptor complexes created on an optical biosensor surface, Protein Sci. 5 (1996) 2468.
[23] D.G. Myszka, T.A. Morton, M.L. Doyle, I.M. Chaiken, Kinetic analysis of a protein antigen–antibody interaction limited by mass transport on an optical biosensor, Biophys. Chem. 64 (1997) 127.